

Option Pricing under Heston Stochastic Volatility Model using Discontinuous Galerkin Finite Elements

Sinem Kozpınar^a, Murat Uzunca^a, Yeliz Yolcu Okur^a, Bülent Karasözen^{a,b}

^a*Institute of Applied Mathematics, Middle East Technical University, 06800 Ankara, Turkey*

^b*Department of Mathematics, Middle East Technical University, 06800 Ankara, Turkey*

Abstract

We consider interior penalty discontinuous Galerkin finite element (dGFEM) method for variable coefficient diffusion-convection-reaction equation to discretize the Heston PDE for the numerical pricing of European options. The mixed derivatives in the cross diffusion term are handled in a natural way compared to the finite difference methods. The advantages of dGFEM space discretization and Cranck-Nicolson method with Rannacher smoothing as time integrator for Heston model with non-smooth initial and boundary conditions are illustrated in several numerical examples for European call, butterfly spread and digital options. The convection dominated Heston PDE for vanishing volatility is efficiently solved utilizing the adaptive dGFEM algorithm. Numerical experiments illustrate that dGFEM is highly accurate and very efficient for pricing financial options.

Keywords: Option pricing, Heston model, discontinuous Galerkin method, adaptive grid

2000 MSC: 65M60, 91B25, 91G80

1. Introduction

The valuation of options are of utmost importance to be able to offset the risk arising from the unexpected price changes in the financial markets. Especially, international investors may incur considerable financial losses due to the fluctuations in the currency prices. Therefore, options on foreign exchange rate are commonly used to mitigate this vulnerability. In this paper, we focus on the pricing of European call, butterfly spread and digital options which are popular among the practitioners.

Since the value of an option is affected by the performance of its underlying, it becomes crucial to examine the price dynamics of the considered security.

Email addresses: ksinem@metu.edu.tr (Sinem Kozpınar), uzunca@gmail.com (Murat Uzunca), yyolcu@metu.edu.tr (Yeliz Yolcu Okur), bulent@metu.edu.tr (Bülent Karasözen)

The celebrated Black-Scholes model [1] is unsuccessful in predicting the volatility smirk due to the assumption of constant volatility. In particular, the model gives poor results for the options on exchange rate [2]. This important shortcoming can be overcome by regarding volatility as a source of randomness as suggested in Heston stochastic volatility model. Under Heston framework, the volatility is treated as a square-root process which enables us to obtain more accurate prices for the European currency options [3]. Indeed, assuming the volatility of the exchange rate is non-constant over time seems a more realistic approach in today's financial markets. Albeit Heston model provides a semi analytical solution for European vanilla options, numerical methods are generally required especially for more complex options.

Option pricing problems are usually solved with the Monte Carlo methods. Although its implementation is straightforward, it requires large number of realizations to achieve high accuracy. Moreover, only one option price can be evaluated for a given initial data. Therefore, the simulations can be too costly which leads us to the discretization methods based on the solution of partial differential equations (PDEs). Option pricing problems under Heston model can be represented as a two-dimensional diffusion-convection-reaction PDE with variable coefficients [3, 4].

In the Heston PDE, the diffusion matrix contains cross-diffusion terms as a result of the correlation between the volatility and the underlying security. Additionally, the initial and boundary data are non-smooth for different options. Therefore, the numerical solution of the Heston PDE is more challenging than the constant coefficient diffusion-convection-reaction equations. The most commonly used method for option pricing is the finite-differences (FDs). Alternating direction implicit (ADI) FD [5, 6] and compact FD schemes [7, 8] are constructed for efficient and accurate discretization of the mixed derivatives in the cross diffusion term, which require sufficiently smooth initial and boundary conditions. The first application of the finite element method (FEM) for option pricing under Heston model goes back to 2000 [9]. The radial basis [10] and spectral methods [11] for option pricing models are more accurate than the FD methods, but have the drawback of requiring the inversion of full system matrices.

In this paper, we apply the symmetric interior penalty discontinuous Galerkin (SIPG) [12, 13] method with upwinding for the convection part [14] to solve Heston's option pricing model for European, butterfly spread and digital options. The discontinuous Galerkin finite element methods (dGFEM) emerged as an alternative to the classical continuous finite element methods in the last twenty years. The basis functions in dGFEM are discontinuous along the inter-element boundaries in contrast to the classical FEMs. The dGFEM has a number of desirable properties like the weakly enforcement of the boundary conditions, hp-refinement (space and order) and ease of parallelization. The stability of discontinuous Galerkin (dG) methods are handled via the penalty term which penalizes the jumps of the solution on the element boundaries in contrast to the classical stabilized FEMs such as streamline upwind/Petrov-Galerkin (SUPG) method with additional stabilization terms. We want to remark that recently

different dG methods are applied for option pricing models [15, 16].

An interesting feature of Heston model is the occurrence of sharp layers or discontinuities for vanishing volatility. In the case of European call options, for instance, extremely high foreign interest rates makes the problem convection-dominated [6] when the underlying volatility is very small. In such cases, the naive approach is to refine the spatial mesh uniformly, which increases the degrees of freedom and refines the mesh unnecessarily in regions where the solutions are smooth. In FD methods, predefined non-uniform grids [5, 6, 7] are used to resolve accurately the discontinuities or the sharp layers. In practice, the location of the interior or boundary layers for convection dominated problems are usually not known a priori. Adaptive FEMs can detect the layers using a posteriori error estimators by refining the mesh locally. Due to the local nature of the basis functions of the dGFEMs, the sharp layers and the singularities of the solution can be detected easily using the adaptive techniques [17] which are robust, i.e. independent of the Péclet number (ratio of convection to diffusion).

Option pricing models have non-smooth initial data, with the discontinuous first derivatives of the payoff functions. The most popular time discretization method in option pricing is the Crank-Nicolson method, which leads undesired oscillations for non-smooth initial data. The instability of the Crank-Nicolson method is remedied by applying in the first four steps the implicit backward Euler method and then continuing with Crank-Nicolson method as time integrator, known as Rannacher smoothing [18]. Rannacher smoothing was used for different option pricing models [19, 20], which we apply here to the Heston model.

The paper is organized as follows: In the next section, we introduce Heston's model for option pricing, and give strong and variational forms of Heston PDE. Space discretization via SIPG method and time discretization by Crank-Nicolson method with Rannacher smoothing are described in Section 3. In Section 4, we present numerical results for the valuation of European call, butterfly spread and digital call options. We also solve a convection dominated problem for European call options using adaptive dGFEM. The paper ends with some conclusions.

2. Heston model

The Heston stochastic volatility model suppose that the volatility of the underlying security is driven by a square-root process [3]. Due to this assumption, the model is successful in modeling the smile effect observed in the option prices. Another main advantage of the model is that a semi-analytical price can be easily derived for the European vanilla options, which makes the model more favorable for practitioners. On the other hand, like the Monte-Carlo method, only a single value of the option can be evaluated for a given data.

In Section 2.1, we describe Heston dynamics, and give the semi-analytical solutions for the value of European vanilla options. In Section 2.2, Heston's two-dimensional diffusion-convection-reaction equation with variable coefficients is

presented. The variational formulation is introduced in Section 2.3, which is needed for the implementation of dGFEM in the text examples.

2.1. The Model Dynamics

In the Heston stochastic volatility model, the value of the underlying security S_t is governed by the stochastic differential equation [3]

$$dS_t = (r_d - r_f)S_t dt + \sqrt{v_t}S_t dW_t^S, \quad (1)$$

and the variance v_t follows the square-root process

$$dv_t = \kappa(\theta - v_t)dt + \sigma\sqrt{v_t}dW_t^v, \quad (2)$$

where W_t^S and W_t^v are correlated standard Brownian motions such that

$$\mathbb{E}^*[dW_t^S dW_t^v] = \rho dt,$$

with ρ being a constant correlation coefficient. Here, r_d is the domestic interest rate, r_f is the foreign interest rate, κ is the mean reversion rate, θ is the long-run mean level of v_t , and σ is the volatility of the volatility (vol of vol). If the parameters in (2) satisfy the well-known Feller condition $2\kappa\theta \geq \sigma^2$, the variance process v_t turns out to be strictly positive, which is fulfilled in most cases.

Let $V^C(t, v, S)$ be the price of a European call option at time t with an exercise price K and maturity T . Considering the dynamics defined in (1)-(2), the semi-analytical solution for the price $V^C(t, v, S)$ is given by [3, 21]:

$$V^C(t, v, S) = S_t e^{-r_f \tau} Q_1 - K e^{-r_d \tau} Q_2, \quad (3)$$

where $\tau = T - t$ denotes the time to maturity and for $k = 1, 2$

$$\begin{aligned} Q_k &= \frac{1}{2} + \frac{1}{\pi} \int_0^\infty \operatorname{Re} \left[\frac{e^{-i\omega \ln(K)}}{i\omega} f_k(\omega; \ln(S), v) \right] d\omega, \\ f_k(\omega; \ln(S), v) &= \exp\{C_k(\tau, \omega) + D_k(\tau, \omega)v + i\omega \ln(S)\}, \\ C_k(\tau, \omega) &= (r_d - r_f)i\omega\tau + \frac{\kappa\theta}{\sigma^2} \left[(b_k - \rho\sigma i\omega + d_k)\tau - 2 \ln \left(\frac{1 - h_k e^{d_k \tau}}{1 - h_k} \right) \right], \\ D_k(\tau, \omega) &= \frac{b_k - \rho\sigma i\omega + d_k}{\sigma^2} \left(\frac{1 - e^{d_k \tau}}{1 - h_k e^{d_k \tau}} \right), \\ h_k &= \frac{b_k - \rho\sigma i\omega + d_k}{b_k - \rho\sigma i\omega - d_k}, \\ d_k &= \sqrt{(\rho\sigma i\omega - b_k)^2 + (-1)^k \sigma^2 i\omega + \sigma^2 \omega^2}, \\ b_k &= (k - 2)\rho\sigma + \kappa. \end{aligned}$$

Analogously, the price of the put option $V^P(t, v, S)$ can be stated as

$$V^P(t, v, S) = S_t e^{-r_f \tau} (Q_1 - 1) + K e^{-r_d \tau} (1 - Q_2), \quad (4)$$

resulting from the put-call parity.

Remark 1. One can also derive a semi-analytical solution for the price of the digital call options. By considering the same arguments used for European vanilla options, the semi-analytical solution for the price of a digital call option can be expressed as [22]:

$$V^D(t, v, S) = e^{-r_d \tau} Q_2, \quad (5)$$

where $V^D(t, v, S)$ is the price of the digital call option with strike price K and maturity T .

2.2. Heston model as parabolic PDE

As a direct application of Feynman-Kac theorem, the no-arbitrage price of a European option under Heston model can be characterized by a two-dimensional diffusion-convection-reaction equation with variable coefficients. Let $V(t, v_t, S_t)$ be the price of a European option at time t and let $g(v_T, S_T)$ denote the payoff received at maturity T . Then, the option price $V(t, v_t, S_t)$ under Heston model satisfies the following linear two-dimensional variable coefficient diffusion-convection-reaction equation [3, 4]

$$\frac{\partial V}{\partial t} + \mathcal{J}_t^S V - r_d V = 0, \quad (6)$$

with the terminal condition

$$V(T, v_T, S_T) = g(v_T, S_T),$$

where $v_t > 0$, $S_t > 0$, $t \in [0, T]$, and

$$\mathcal{J}_t^S V = \frac{1}{2} S^2 v \frac{\partial^2 V}{\partial S^2} + (r_d - r_f) S \frac{\partial V}{\partial S} + \rho \sigma S v \frac{\partial^2 V}{\partial v \partial S} + \frac{1}{2} \sigma^2 v \frac{\partial^2 V}{\partial v^2} + \kappa(\theta - v) \frac{\partial V}{\partial v}.$$

Applying the so called log transformation $x = \log(S/K)$ and $\tau = T - t$ with $U(\tau, v, x) = V(T - \tau, v, K e^x)$, PDE (6) is converted to the following equation

$$\frac{\partial U}{\partial \tau} - \mathcal{J}_\tau^x U + r_d U = 0, \quad (7)$$

where $v > 0$, $x \in (-\infty, \infty)$, $\tau \in [0, T]$, and

$$\mathcal{J}_\tau^x U = \frac{1}{2} v \frac{\partial^2 U}{\partial x^2} + (r_d - r_f - \frac{1}{2} v) \frac{\partial U}{\partial x} + \rho \sigma v \frac{\partial^2 U}{\partial v \partial x} + \frac{1}{2} \sigma^2 v \frac{\partial^2 U}{\partial v^2} + \kappa(\theta - v) \frac{\partial U}{\partial v}.$$

Note that due to the substitution $\tau = T - t$, PDE (7) can also be regarded as a forward equation with the following initial condition

$$U^0 := U(0, v, x) = g(v, K e^x).$$

We consider an open bounded domain Ω with the boundary $\Gamma = \Gamma_D \cup \Gamma_N$, where on Γ_D the Dirichlet and on Γ_N the Neumann boundary conditions

are prescribed, respectively. Then, the log transformed PDE given in (7) is expressed as a diffusion-convection-reaction equation

$$\frac{\partial U}{\partial \tau} - \nabla \cdot (A \nabla U) + b \cdot \nabla U + r_d U = 0 \quad \text{in } (0, T) \times \Omega, \quad (8a)$$

$$U(t, \mathbf{z}) = U^D(t, \mathbf{z}) \quad \text{on } (0, T) \times \Gamma_D, \quad (8b)$$

$$A \nabla U(t, \mathbf{z}) \cdot \mathbf{n} = U^N(t, \mathbf{z}) \quad \text{on } (0, T) \times \Gamma_N, \quad (8c)$$

$$U(0, \mathbf{z}) = U^0(\mathbf{z}) \quad \text{in } \{0\} \times \Omega, \quad (8d)$$

where \mathbf{n} is the outward unit normal vector, $\mathbf{z} = (v, x)^T$, throughout this paper, is the spatial element. In (8), the diffusion matrix and convective field are given by

$$A = \frac{1}{2}v \begin{pmatrix} \sigma^2 & \rho\sigma \\ \rho\sigma & 1 \end{pmatrix} \quad \text{and} \quad b = v \begin{pmatrix} \kappa \\ \frac{1}{2} \end{pmatrix} + \begin{pmatrix} -\kappa\theta + \frac{1}{2}\sigma^2 \\ -(r_d - r_f) + \frac{1}{2}\rho\sigma \end{pmatrix}.$$

Remark 2. Although, the transformed PDE (7) is defined on the computational domain $(0, \infty) \times (-\infty, \infty)$, dGFEM must be performed on a bounded spatial region $\Omega = (v_{min}, v_{max}) \times (x_{min}, x_{max})$ for the numerical simulations.

2.3. Variational form of Heston's model

We introduce the weak formulation of Heston's model as parabolic convection-diffusion-reaction equation (8). Let $L^2(\Omega)$ be the space consisting of all square integrable functions on Ω , $H^1(\Omega)$ denote the Hilbert space of all functions having square integrable first-order partial derivatives, and $H_0^1(\Omega) = \{w \in H^1(\Omega) : w = 0 \text{ on } \Gamma_D\}$. The weak form of (8) is obtained by multiplying with a test function $w \in H_0^1(\Omega)$ and integrating by parts over the domain Ω . Then, for a.e. $t \in (0, T]$, we seek a solution $U(t, v, x) \in H_D^1(\Omega) = \{U \in H^1(\Omega) : U = U^D \text{ on } \Gamma_D\}$ satisfying

$$\int_{\Omega} \frac{\partial U}{\partial \tau} w d\mathbf{z} + a(U, w) = \int_{\Gamma_N} U^N w ds \quad \forall w \in H_0^1(\Omega), \quad (9a)$$

$$\int_{\Omega} U(0, \mathbf{z}) w d\mathbf{z} = \int_{\Omega} U^0 w d\mathbf{z} \quad \forall w \in H_0^1(\Omega), \quad (9b)$$

where ds is the arc-length element on the boundary. In (9), $a(u, w)$ is the bilinear form given by

$$a(u, w) = \int_{\Omega} (A \nabla U \cdot \nabla w + b \cdot \nabla U w + r_d U w) d\mathbf{z}, \quad \forall w \in H_0^1(\Omega).$$

We assume that the matrix A is positive definite, i.e. $v > 0$ and $\rho \in (-1, 1)$ which is usually satisfied.

There exist constants C , c_1 and c_2 for all u and w , so that the bilinear form $a(u, w)$ is continuous and weakly coercive [9]:

$$\begin{aligned} |a(u, w)| &\leq C \|u\|_{H^1(\Omega)} \|w\|_{H^1(\Omega)}, & u, w &\in H^1(\Omega) \\ a(t; u, w) &\geq c_1 \|w\|_{H^1(\Omega)} - c_2 \|w\|_{L_2(\Omega)}^2, & w &\in H^1(\Omega) \end{aligned}$$

The first inequality accounts to the continuity of the bilinear form and the second is the Gårding inequality. The weakly coercive bilinear form $a(\cdot, \cdot)$ can be transformed into a coercive one using the substitution $\tilde{u} = e^{c_2 t} u(x, t)$ [23, Sec. 1.3.3]. Then, there exist a unique solution and the following energy estimate holds

$$\max_{t \in [0, T]} \|u(t)\|_{L^2}^2 + c_1 \int_0^T \|u(t)\|_H^2 \leq \|u(0)\|_{L^2}^2 + \frac{1}{c_1} \int_0^T \|f(t)\|_2^2.$$

3. Symmetric interior penalty discontinuous Galerkin (SIPG) method

The symmetric interior penalty Galerkin (SIPG) method is the commonly used dG method, which enforces boundary conditions weakly [13]. Let the mesh $\xi_h = \{K\}$ be a partition of the domain Ω into a family of shape regular elements (triangles). We set the mesh-dependent finite dimensional solution and test function space by

$$W_h = W_h(\xi_h) = \{w \in L^2(\Omega) : w|_K \in \mathbb{P}_k(K), \forall K \in \xi_h\} \not\subset H_0^1(\Omega),$$

where the functions in W_h are discontinuous along the inter-element boundaries. These discontinuities leads to the fact that on an interior edge e shared by two neighboring triangles K_i and K_j , there are two different traces from either triangles. Thus, for convenient, we define the jump and average operators of a function $w \in W_h$ on e by

$$[[u]] := u|_{K_i} \mathbf{n}_{K_i} + u|_{K_j} \mathbf{n}_{K_j}, \quad \{u\} := \frac{1}{2}(u|_{K_i} + u|_{K_j}).$$

On a boundary edge $e \subset \partial\Omega$, we set $[[u]] := u|_K \mathbf{n}$ and $\{u\} := u|_K$. In addition, we form the sets of inflow and outflow edges by

$$\Gamma^- = \{\mathbf{z} \in \partial\Omega : \mathbf{b}(v) \cdot \mathbf{n}(v, x) < 0\}, \quad \Gamma^+ = \partial\Omega \setminus \Gamma^-,$$

$$\partial K^- = \{\mathbf{z} \in \partial K : \mathbf{b}(v) \cdot \mathbf{n}_K(v, x) < 0\}, \quad \partial K^+ = \partial K \setminus \partial K^-,$$

where \mathbf{n}_K denotes the outward unit vector on an element boundary ∂K . Moreover, we denote by Γ_h^0 and Γ_h^D the sets of interior and Dirichlet boundary edges, respectively so that the union set $\Gamma_h = \Gamma_h^0 \cup \Gamma_h^D$. Then, in space SIPG discretized semi-discrete system of the PDE (8) reads as: for a.e. $t \in (0, T]$, for all $w_h \in W_h$, find $U_h := U_h(t, \mathbf{z}) \in W_h$ such that

$$\int_{\Omega} \frac{\partial U_h}{\partial t} w_h d\mathbf{z} + a_h(t; U_h, w_h) = l_h(w_h), \quad (10a)$$

$$\int_{\Omega} U_h(0, \mathbf{z}) w_h d\mathbf{z} = \int_{\Omega} U^0 w_h d\mathbf{z}, \quad (10b)$$

with the (bi)linear forms:

$$\begin{aligned}
a_h(t; U_h, w_h) &= \sum_{K \in \xi_h} \int_K (A \nabla U_h \cdot \nabla w_h + b \cdot \nabla U_h w_h + r_d U_h w_h) d\mathbf{z} \\
&\quad + \sum_{e \in \Gamma_h} \int_e \left(\frac{\sigma_e}{h_e} \llbracket U_h \rrbracket \cdot \llbracket w_h \rrbracket - \{A \nabla w_h\} \llbracket U_h \rrbracket - \{A \nabla U_h\} \llbracket w_h \rrbracket \right) ds \\
&\quad + \sum_{K \in \xi_h} \left(\int_{\partial K^- \setminus \partial \Omega} b \cdot \mathbf{n}_K (U_h^{out} - U_h) w_h ds - \int_{\partial K^- \cap \Gamma^-} b \cdot \mathbf{n}_K U_h w_h ds \right), \\
l_h(w_h) &= \sum_{e \in \Gamma_h^N} \int_e U^N w_h d\mathbf{z} + \sum_{e \in \Gamma_h^D} \int_e U^D \left(\frac{\sigma_e}{h_e} w_h - A \nabla w_h \right) ds \\
&\quad - \sum_{K \in \xi_h} \int_{\partial K^- \cap \Gamma^-} b \cdot \mathbf{n}_K U^D w_h ds,
\end{aligned}$$

where U_h^{out} denotes the trace of U_h on an edge e from outside the triangle K .

The penalty parameter σ_e should be selected sufficiently large to ensure the coercivity of the bilinear form [13, Sec. 27.1]. It ensures that the dG stiffness matrix is positive definite. At the same time it should not be too large since the stiffness matrix becomes ill-conditioned for large penalty parameters. Here we follow [24] to estimate the penalty parameter, above a threshold value the bilinear form is coercive and the scheme is stable and convergent. From the uniform ellipticity (positive definiteness) of the diffusion matrix $A(v)$, it follows that there exist two constants d_0 and d_1 such that the following inequality holds

$$d_0 z^T z \leq z^T A z \leq d_1 z^T z, \quad \forall z \in \mathbb{R}^2.$$

Then, one can obtain the penalty parameter σ_e as [24]

$$\sigma_e = \frac{3d_1^2}{d_0} k(k+1) \cot \theta, \quad \forall e \in \Gamma_h^0, \quad \sigma_e = \frac{6d_1^2}{d_0} k(k+1) \cot \theta, \quad \forall e \in \Gamma_h^D,$$

where θ denotes the smallest angle over all triangles in ξ_h .

The solution of SIPG semi-discretized Heston model (10) is given as

$$U_h(t, \mathbf{z}) = \sum_{m=1}^N \sum_{j=1}^{n_q} u_j^m(t) \varphi_j^m(\mathbf{z}), \quad (12)$$

where φ_j^m and u_j^m , $j = 1, \dots, n_q$, $m = 1, \dots, N$, are the basis functions spanning the space W_h and the unknown coefficients, respectively. The number n_q denotes the local dimension of each DG element with $n_q = (q+1)(q+2)/2$ for 2D problems, and N is the number of dG elements (triangles). Substituting (12) into (10) and choosing $v = \varphi_i^k$, $i = 1, \dots, n_q$, $k = 1, \dots, N$, we obtain the following semi-linear system of ordinary differential equations (ODEs) for the unknown coefficient vector $\mathbf{u} = (u_1^1, \dots, u_{n_q}^1, u_1^2, \dots, u_1^N, \dots, u_{n_q}^N)^T$

$$M_h \mathbf{u}_t + A_h \mathbf{u} = \mathbf{l}_h, \quad (13)$$

where M is the mass matrix and A_h is the stiffness matrix, with the entries $(M_h)_{ij} = (\varphi^j, \varphi^i)_\Omega$ and $(A_h)_{ij} = a_h(\cdot; \varphi^j, \varphi^i)$, $1 \leq i, j \leq n_q \times N$. For the time discretization, we consider a subdivision of $[0, T]$ into J time intervals $I_n = (t^{n-1}, t^n]$ of length Δt_n , $n = 1, 2, \dots, J$, with $t^0 = 0$.

We solve (13) with Rannacher smoothing [18] applying four steps backward Euler method with the step size $\Delta t/2$ and continuing with the Crank-Nicolson method with the step size Δt , thus the same coefficient matrix is formed [19]:

$$\begin{aligned} \left(M_h + \frac{\Delta t}{2} A_h\right) \mathbf{u}^{n+1} &= M_h \mathbf{u}^n + \frac{\Delta t}{2} \mathbf{l}_h^{n+1}, & n = 0, 1, 2, 3, \\ \left(M_h + \frac{\Delta t}{2} A_h\right) \mathbf{u}^{n+1} &= \left(M_h - \frac{\Delta t}{2} A_h\right) \mathbf{u}^n + \frac{\Delta t}{2} (\mathbf{l}_h^n + \mathbf{l}_h^{n+1}), & n = 4, \dots \end{aligned} \quad (14)$$

The coefficient matrix is factorized by LU decomposition at the initial time step and used in all successive time steps, which makes the time integration efficient.

4. Numerical results

In this section, Heston PDE is solved numerically for different types of options to show the accuracy and efficiency of the SIPG method.

As the first test example, we consider European call options for which semi-analytical solutions can be obtained. The second test example is the convection dominated European call option pricing model solved by the adaptive dGFEM. It is widely known that Heston PDE can be viewed as convection-dominated for low volatilities; the numerical solutions exhibit oscillations around $v \approx 0$. In the case of European call options, the Heston PDE becomes convection dominated especially for high foreign interest rates. We show also the performance of the SIPG discretization with Rannacher smoothing in time for butterfly and digital options with more non-smooth initial data than the European option.

It is worth mentioning that there is no a consensus in the literature regarding the boundary conditions [25]. The main contentious issue is that some proposes to impose a boundary condition at $v = 0$ if the Feller-condition is disregarded, see for instance [9, 26, 19]. From the computational standpoint, when the parameters κ , σ and θ of the squared-root process v_t are not chosen according to condition $2\kappa\theta \geq \sigma^2$, v_t can become zero for some points in time. Thereby, an appropriate boundary condition at $v = 0$ is required to solve Heston's diffusion-convection-reaction equation (8). On the other hand, from the financial standpoint, the Feller condition is not violated; therefore, some discuss that it suffices to define a boundary condition at x_{\min} , x_{\max} and v_{\max} . In that case, PDE (8) is subject to an outflow boundary at $v = 0$, see e.g. [3, 5, 10]. The other controversy stems from the fact that one can find many different types of boundary conditions when pricing an option. Therefore, it is not certain at which boundary condition Heston's PDE should be used to achieve highly accurate solutions. For a detailed discussion on boundary conditions in option pricing, we refer to [25].

4.1. Test example 1: Option pricing with Dirichlet boundary conditions

To illustrate that SIPG provides accurate solutions for Heston's model, we consider the valuation of European call options due to the fact that its semi-analytical benchmark price can easily be derived, as mentioned in Section 2.1.

Let $U(\tau, v, x)$ be the price of a European call option at time τ , and let $g(v, Ke^x)$ denotes its payoff

$$g(v, Ke^x) = (Ke^x - K)^+,$$

with K being the strike price of the option. We consider the diffusion-convection-reaction equation (8) under the non-homogenous Dirichlet boundary conditions [26]:

$$\begin{aligned} U(\tau, v_{\min}, x) &= (Ke^{x-r_f\tau} - Ke^{-r_d\tau})^+, \\ U(\tau, v_{\max}, x) &= Ke^{x-r_f\tau}, \\ U(\tau, v, x_{\min}) &= 0, \\ U(\tau, v, x_{\max}) &= (Ke^{x_{\max}-r_f\tau} - Ke^{-r_d\tau})^+, \end{aligned} \tag{15}$$

with the initial condition $U(0, v, x) = (Ke^x - K)^+$. We note that for numerical simulations, the unbounded computational domain $[0, \infty) \times (-\infty, \infty)$ transformed to a bounded one $\Omega = [0, 4] \times [-2, 2]$ with a mesh and time step size $\Delta v = \Delta x = 0.0625$, $\Delta\tau = 0.01$. The parameters are set as in Table 1 [26].

Table 1: Parameter set for the test example 1

κ	θ	σ	ρ	r_d	r_f	T	S_0	v_0
1.0	0.09	0.4	-0.7	0.05	0.01	1	100	0.25

In Table 2, the numerical solutions obtained by the SIPG are compared with semi-analytical (closed form) solutions given in Section 2.1. As it can be seen from the relative errors in Table 2, SIPG turns out to provide highly accurate prices for the call option with different strike prices. One can also observe from Table 2 that, the SIPG method requires less CPU time (in seconds) than the Monte Carlo method using 10^6 number of sample paths.

Table 2: Comparison with the closed form solutions and Monte Carlo simulation for different strike prices, $\Delta\tau = 0.01$: linear (quadratic) dG elements.

K_c	closed-form solution	relative error Monte Carlo	relative error SIPG	CPU time Monte Carlo	CPU time SIPG
105	15.938	1.05e-03	1.79e-04 (5.33e-05)	224.8	30.2 (82.0)
110	13.857	1.12e-03	1.79e-03 (5.25e-05)	228.4	30.6 (78.8)
115	11.979	1.36e-03	5.16e-04 (1.26e-04)	222.9	28.9 (77.1)
130	7.483	1.62e-03	1.56e-03 (2.05e-04)	224.7	30.5 (82.4)
150	3.701	1.03e-03	5.42e-04 (1.99e-04)	224.0	30.5 (81.9)

4.2. Test example 2: convection dominated European Call option under Heston model

We consider the convection-dominated Heston PDE for European call options [6]. In order to illustrate the effect of large convective terms in the context of option pricing, we present numerical results for the high foreign interest rates. In the literature, for convection dominated option pricing models, usually special predefined non-uniform grids are used for FD methods [5, 6, 7] and for finite volume methods [27].

There are two critical points for the European call options under Heston model. The first one is around $S = K$ where the option is at the money. The other one is near the boundary $v = 0$, at which the oscillations occur due to the large convection coefficients relatively to the diffusion coefficients, making the PDE convection-dominated in this area. The solution of the evolution problems modeled by the convection dominated diffusion-convection-reaction equations has a number of challenges. In one hand, one has to resolve the solution around the interior/boundary layers due to the convection domination. On the other hand, the nature of non-stationary model leads to the resolution of spatial layers to be more critical since the location of the layers may vary as time progresses. In case of convection dominated Heston's model, the location of the layer is not changed as time progresses. Therefore the adaptive grid constructed at the begin of the time integration for the stationary convection-diffusion-reaction equation and it is used in all the succeeding time steps.

The adaptive dGFEM consists of finding a non-uniform mesh $\xi_h := \xi_h^{(s)}$ ($s > 0$) starting from a coarse uniform mesh $\xi_h^{(0)}$ by successive loops of the following sequence:

$$\text{SOLVE} \longrightarrow \text{ESTIMATE} \longrightarrow \text{MARK} \longrightarrow \text{REFINE}$$

Thus, on the s -th iteration, we solve (14) for \mathbf{u}^1 and we obtain U_h^1 on the mesh $\xi_h^{(s-1)}$. Using computed solution U_h^1 , then, the local error indicators are calculated on each triangle $K \in \xi_h^{(s-1)}$, and according to local error indicators, the elements having large error are refined to obtain the new non-uniform mesh $\xi_h^{(s)}$. Here, the key step is the estimation of the local error indicators by use of only computed solution and given problem data (a posteriori). As a posteriori error indicator, we use the robust (independent of the Pélet number) residual based error indicator in [17], derived for a linear stationary diffusion-convection-reaction equation. So, for each element $K \in \xi_h^{(s-1)}$, we define the local error indicators η_K^2 :

$$\eta_K^2 = \eta_{R_K}^2 + \eta_{E_K^0}^2 + \eta_{E_K^D}^2 + \eta_{E_K^N}^2, \quad (16)$$

where η_{R_K} denotes the cell residuals

$$\eta_{R_K}^2 = \rho_K^2 \|(U_h^1 - U_h^0)/\Delta t_1 - \nabla_h \cdot (A(v)\nabla_h U_h^1) + \mathbf{b} \cdot \nabla_h U_h^1 + r_d U_h^1\|_{L^2(K)}^2,$$

while, $\eta_{E_K^0}$, $\eta_{E_K^D}$ and $\eta_{E_K^N}$ stand for the edge residuals coming from the jump of the numerical solution on the interior, Dirichlet boundary and Neumann

boundary edges, respectively, and ρ_K is a positive weight (see [17] for details). The a posteriori error indicator is given by

$$\eta = \left(\sum_{K \in \xi_h^{(0)}} \eta_K^2 \right)^{1/2}.$$

The iteration continues until a prescribed condition $\eta < \epsilon$ is satisfied, producing the fix non-uniform mesh $\xi_h := \xi_h^{(s)}$ to be used in the successive time steps, for some $s \in \mathbb{Z}^+$.

Table 3: Parameter set for the convection dominated problem

κ	θ	σ	ρ	r_d	T	K
1.98937	0.011876	0.33147	0.0258519	$\log(1.0005)$	0.25	123.4

For the numerical experiments, we impose the following boundary conditions proposed in [9]:

$$\begin{aligned} U(\tau, v_{\min}, x) &= Ke^{x-r_f\tau}\Phi(d_+) - Ke^{r_d\tau}\Phi(d_-) \\ U(\tau, v_{\max}, x) &= Ke^{x-r_f\tau} \\ U(\tau, v, x_{\min}) &= \lambda U(\tau, v_{\max}, x_{\min}) + (1-\lambda)U(\tau, v_{\min}, x_{\min}) \\ \frac{\partial}{\partial \nu} U(\tau, v, x_{\max}) &= A \nabla U \cdot \vec{n} = \frac{1}{2} v K e^{x-r_f\tau} \\ U(\tau, v, x) &= (Ke^x - K)^+ \end{aligned}$$

where \vec{n} is the outward normal vector,

$$d_+ = \frac{x + (r_d - r_f + \frac{1}{2}v_{\min})\tau}{\sqrt{v_{\min}\tau}}, \quad d_- = \frac{x + (r_d - r_f - \frac{1}{2}v_{\max})\tau}{\sqrt{v_{\max}\tau}}$$

and $\Phi(x)$ is the cumulative distribution function given as

$$\Phi(x) = \frac{1}{2\pi} \int_{-\infty}^x e^{-y^2/2} dy.$$

The parameters are taken from [6] (see Table 3). We consider a bounded domain $(0.0025, 0.559951) \times (2.990790, 6.640072)$ for the computational purposes. The constant time step size is taken as $\Delta t = 0.0125$. Precisely, we choose $r_f = \log(100)$ to examine the effect of large convective terms in a superior way.

The adaptive solution produces accurate solutions without oscillations using less degrees of freedom (DoFs) (one tenth) (Figure 1 right) than the oscillating solutions for the uniform meshes (Figure 1 left). The layer is also accurately detected by the adaptive algorithm as shown in Figure 2.

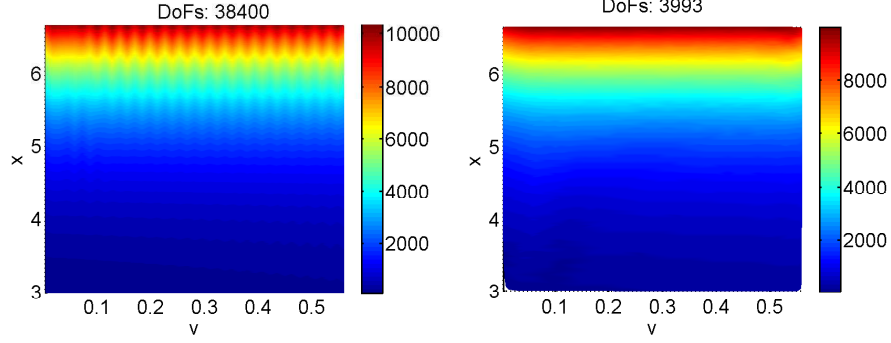


Figure 1: Solution profiles at $\tau = 0$ by a uniform (left) and adaptive mesh (right).

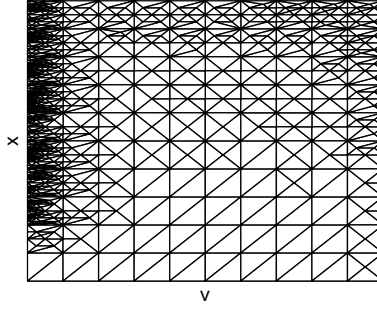


Figure 2: Adaptive mesh.

4.3. Test example 3: Butterfly Call option

This example is chosen for the valuation of butterfly call spreads. A butterfly call spread is a strategy favored by the traders who do not expect significant movements in the underlying value. The spread is created by combining three call options with different strike prices. Precisely, for $K_1 < K_3$, we buy two call options with a strike price K_1 and K_3 , and sell two call options with a strike price $K_2 = (K_1 + K_3)/2$. The payoff function is then given by

$$g(v, Ke^x) = (K_2 e^x - K_1)^+ - 2(K_2 e^x - K_2)^+ + (K_2 e^x - K_3)^+,$$

with $x = \log(S/K_2)$. Note that the payoff function (initial data) is non-differentiable at the strike prices K_1 , K_2 and K_3 .

Let $U(\tau, v, x)$ be the price of a butterfly spread option satisfying Heston's PDE (8) with $x = \log(S/K_2)$. We impose the homogeneous Dirichlet type boundary conditions in the x -direction, as proposed in [10]:

$$U(\tau, v, x_{\min}) = 0, \quad U(\tau, v, x_{\max}) = 0,$$

with an initial condition

$$U(0, v, x) = (K_2 e^x - K_1)^+ - 2(K_2 e^x - K_2)^+ + (K_2 e^x - K_3)^+.$$

Additionally, we apply the homogeneous Neumann boundary conditions in the v -direction:

$$\frac{\partial}{\partial v} U(\tau, v_{\min}, x) = 0, \quad \frac{\partial}{\partial v} U(\tau, v_{\max}, x) = 0.$$

Indeed, when $v \rightarrow 0$ and $v \rightarrow \infty$, it is observed that the price of the underlying security becomes steady [28]. As a result, the value of the spread does not show a sensitivity for the extreme values of volatility.

In analogous to the before mentioned test examples 1 and 2, the computational domain is reduced to a bounded one $(0.0025, 0.559951) \times (-5, 5)$. Parameter set is taken from [9] (see Table 4). The mesh and time step sizes are chosen as $\Delta x = 0.078$, $\Delta v = 0.016$ and $\Delta t = 0.025$.

Figure 3 displays the payoff (left) and price surface (right) of a butterfly spread with $K_1 = 0.1$, $K_2 = 0.5$, $K_3 = 0.9$. As expected, at the strike prices K_1 , K_2 and K_3 the payoff function is non-differentiable. On the other hand, due to the diffusion effect, the non-smoothness seems to be mitigated as $\tau \rightarrow 0.25$. Indeed, the effect of diffusion terms is more significant when the underlying is very volatile. Note that due to the no-arbitrage arguments, the value of this spread can be determined as a combination of the prices of the considered call options.

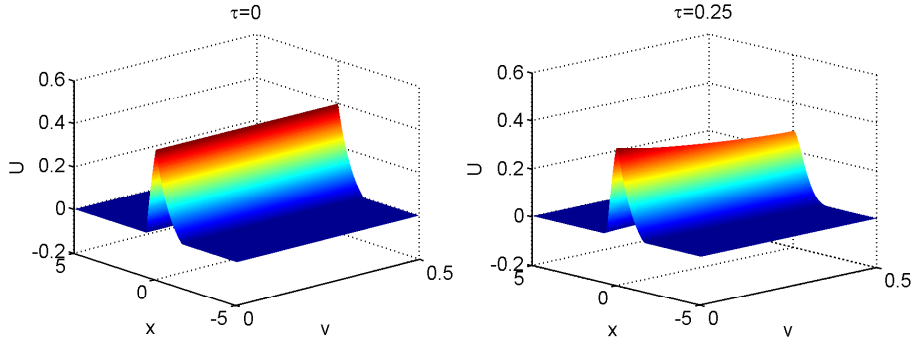


Figure 3: Price profile of a butterfly spread at $\tau = 0$ (left) and at $\tau = 0.25$ (right) with $x = \log(S/K_2)$.

4.4. Test example 4: Digital Call option

Finally, we examine the performance of SIPG with Rannacher smoothing for the digital call options with a discontinuous payoff [22, 28]

$$g(v, K e^x) = \mathbb{1}_{\{K e^x > K\}},$$

Table 4: Parameter set for the test example 3

κ	θ	σ	ρ	r_d	r_f	T	S_0	K	v_0
2.5	0.06	0.5	-0.1	$\log(1.052)$	$\log(1.048)$	0.25	1	1	0.05225

where K is the strike price of the option, which is treated as a barrier level. Precisely, if the stock price reaches the level K at maturity, then the option will be worthless or it will pay 1 unit of money at time T . Let $U(\tau, v, x)$ be the price of a digital call option adhering Heston diffusion-convection-reaction equation (8). Differently from the test example 3, we now impose an inhomogeneous Dirichlet boundary condition at $x = x_{\max}$ [28]:

$$U(\tau, v, x_{\max}) = e^{x_{\max} - r_f \tau}$$

and an initial condition

$$U(0, v, x) = \mathbb{1}_{\{K e^x > K\}}.$$

The idea behind this boundary condition can be given as follows: When the price of the underlying security is very high as compared to the strike price, then the option is worth $e^{x - r_f \tau}$ as reaching to a value of 1 at maturity. Moreover, regarding the boundaries at $v = v_{\min}$ and $v = v_{\max}$, we follow the same financial consideration, as for butterfly spread [28].

As in the test example 3, the numerical computations are performed under the bounded domain $(0.0025, 0.559951) \times (-5, 5)$ with the same mesh and time step sizes, i.e. $\Delta x = 0.078$, $\Delta v = 0.016$ and $\Delta t = 0.025$.

Figure 4 illustrates the payoff (left) and price surface (right) of the considered digital call option. It is apparent from figure that the payoff function is bended at $x = 0$ due to the non-smoothness. On the other hand, the price function seems to be smoother as a result of the diffusion effect. Indeed, the effect of the diffusion term is more visible for large volatilities.

In Table 5, we compare the relative errors of Crank-Nicolson and Crank-Nicolson with Rannacher smoothing for linear dG elements with $v_0 = 0.05225$ and $S_0 = 1$, where the reference solution 0.483827, obtained by the semi-analytical formula in Section 2.1. Here, N_v and N_x denotes the number of partitions in the v and x -direction, respectively. It is apparent that the Rannacher smoothing produces by far more accurate solutions than the Crank-Nicolson method especially for fine grids.

5. Conclusions

The numerical results provided in Section 4 demonstrate that dGFEMs are a very effective and accurate method for solving option pricing problems under Heston model. The non-smooth boundary and initial conditions for various option pricing models can be handled in a natural way by the dGFEMs in combination with the Rannacher smoothing in time, as compared with other discretization techniques used in the literature for option pricing.

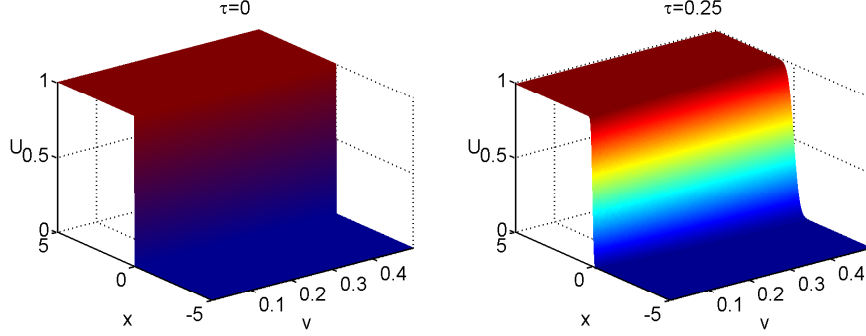


Figure 4: Price profile of a European digital call option at $\tau = 0$ (left) and at $\tau = 0.25$ (right) with $x = \log(S/K)$.

Table 5: Relative errors for digital call option

		Crank-Nicolson		Rannacher smoothing	
N_v	N_x	value	relative error	value	relative error
8	16	0.524935	8.50e-02	0.524910	8.49e-02
16	64	0.494234	2.15e-02	0.496226	2.56e-02
32	128	0.368798	2.38e-01	0.484065	4.93e-04
64	256	0.554879	1.47e-01	0.483568	5.34e-04

References

- [1] F. Black, M. Scholes, The pricing of options and corporate liabilities, The journal of political economy (1973) 637–654.
- [2] A. Melino, S. M. Turnbull, Pricing foreign currency options with stochastic volatility, Journal of Econometrics 45 (1) (1990) 239–265.
- [3] S. L. Heston, A closed-form solution for options with stochastic volatility with applications to bond and currency options, Review of Financial Studies 6 (2) (1993) 327–343. doi:10.1093/rfs/6.2.327.
- [4] A. Lipton, Mathematical methods for foreign exchange: A financial engineer’s approach, World Scientific, 2001.
- [5] K. J. In’T Hout, S. Foulon, ADI finite difference schemes for option pricing in the Heston model with correlation, International Journal of Numerical Analysis and Modeling 7 (2) (2010) 303–320.
- [6] T. Kluge, Pricing derivatives in stochastic volatility models using the finite difference method, Master’s thesis, Technische Universität Chemnitz (2002).

- [7] B. Düring, M. Fournié, C. Heuer, High-order compact finite difference schemes for option pricing in stochastic volatility models on non-uniform grids, *Journal of Computational and Applied Mathematics* 271 (2014) 247 – 266. doi:10.1016/j.cam.2014.04.016.
- [8] D. Tangman, A. Gopaul, M. Bhuruth, Numerical pricing of options using high-order compact finite difference schemes, *Journal of Computational and Applied Mathematics* 218 (2) (2008) 270–280. doi:10.1016/j.cam.2007.01.035.
- [9] G. Winkler, T. Apel, U. Wystup, Valuation of options in Hestons stochastic volatility model using finite element methods, *Foreign Exchange Risk* (2001) 283–303.
- [10] L. V. Ballestra, G. Pacelli, Pricing European and American options with two stochastic factors: A highly efficient radial basis function approach, *Journal of Economic Dynamics and Control* 37 (6) (2013) 1142 – 1167. doi:10.1016/j.jedc.2013.01.013.
- [11] E. Pindza, K. C. Patidar, E. Ngounda, Implicit-explicit predictor-corrector methods combined with improved spectral methods for pricing European style vanilla and exotic options, *Electron. Trans. Numer. Anal.* 40 (2013) 268–293.
- [12] D. N. Arnold, F. Brezzi, B. Cockburn, L. D. Marini, Unified analysis of discontinuous Galerkin methods for elliptic problems, *SIAM Journal on Numerical Analysis* 39 (5) (2002) 1749–1779. doi:10.1137/S0036142901384162.
- [13] B. Rivière, *Discontinuous Galerkin methods for solving elliptic and parabolic equations, Theory and implementation*, SIAM, 2008.
- [14] B. Ayuso, L. D. Marini, Discontinuous Galerkin methods for advection-diffusion-reaction problems, *SIAM Journal on Numerical Analysis* 47 (2) (2009) 1391–1420. doi:10.1137/080719583.
- [15] J. Hozman, Valuing barrier options using the adaptive discontinuous Galerkin method, in: *Programs and algorithms of numerical mathematics 16*, Acad. Sci. Czech Repub. Inst. Math., Prague, 2013, pp. 94–99.
- [16] D. P. Nicholls, A. Sward, A discontinuous Galerkin method for pricing American options under the constant elasticity of variance model, *Communications in Computational Physics* 17 (2015) 761–778. doi:10.4208/cicp.190513.131114a.
- [17] D. Schötzau, L. Zhu, A robust a-posteriori error estimator for discontinuous Galerkin methods for convection-diffusion equations, *Applied Numerical Mathematics* 59 (9) (2009) 2236 – 2255. doi:10.1016/j.apnum.2008.12.014.

- [18] R. Rannacher, Finite element solution of diffusion problems with irregular data, *Numerische Mathematik* 43 (2) (1984) 309–327. doi:10.1007/BF01390130.
- [19] S. Ikonen, J. Toivanen, Efficient numerical methods for pricing American options under stochastic volatility, *Numerical Methods for Partial Differential Equations* 24 (1) (2008) 104–126. doi:10.1002/num.20239.
- [20] D. Pooley, K. Vetzal, P. Forsyth, Convergence remedies for non-smooth payoffs in option pricing, *J. Comput. Finance* 6 (2003) 25–40.
- [21] F. D. Rouah, *The Heston model and its extensions in MATLAB and C#*, John Wiley & Sons, 2013.
- [22] V. L. Lazar, Pricing digital call option in the Heston stochastic volatility model, *Studia Univ. Babeş-Bolyai Math.* 48 (3) (2003) 83–92.
- [23] P. Solin, *Partial Differential Equations*, John Wiley & Sons, Inc., 2005, Ch. 1, pp. 1–44. doi:10.1002/0471764108.ch1.
- [24] Y. Epshteyn, B. Rivière, Estimation of penalty parameters for symmetric interior penalty Galerkin methods, *J. Comput. Appl. Math.* 206 (2007) 843–872.
- [25] S.-P. Zhu, W.-T. Chen, A predictor–corrector scheme based on the ADI method for pricing American puts with stochastic volatility, *Computers & Mathematics with Applications* 62 (1) (2011) 1–26.
- [26] X. Chen, J. Burkardt, M. Gunzburger, High accuracy finite element methods for option pricing under Heston’s stochastic volatility model, *Florida State University* (2014).
- [27] G. I. Ramirez-Espinoza, M. Ehrhardt, Conservative and finite volume methods for the convection-dominated pricing problem, *Advances in Applied Mathematics and Mechanics* 5 (2013) 759–790.
- [28] R. England, *The use of numerical methods in solving pricing problems for exotic financial derivatives with a stochastic volatility*, Ph.D. thesis, M. Sc. Thesis, University of Reading (2006).